Hydrodynamic Force Comparison on Multi-Hull, Monohull and Single-to-Twin After Ship Hull (STASH) Based on Seakeeping Criteria

G.A.P. Poundra[a*], B.K. Aditya[a], S. Widiyanto[a]

[a]*Universitas Hang Tuah, Jl. Arif Rahman Hakim no. 150, Surabaya 60111, Indonesia*

Corresponding author: poundra.akira@gmail.com

Abstract

An investigation into the hydrodynamic force and seakeeping of single-to-twin after ship hull (STASH) and multi-hull geometry was done successfully. STASH is characterized by its monohull-shaped design in the fore part and twin hull in the rear part creating unique performance, especially seakeeping which being the focus study to provide seaworthiness. The method of accomplishing this study was through computer simulation using Maxsurf: Motion for seakeeping and hydrodynamic force analysis. The overall results were compared with published data and mathematical models for validation purposes. The results are believed to be useful for the development of the ship design and performance.

Keywords: Hydrodynamic force; Maxsurf; Multi-hull; Seakeeping; STASH

1. Introduction

The assessment of ship's ability to withstand the dynamic forces exerted by ocean waves (seakeeping) occupies a crucial role in the design process, encompassing both conceptual and structural aspects. The significance arises from the vessel's exposure to the risk of accidents during operation (such as collisions, grounding, capsizing, etc.), which may subsequently lead to disruptions in health, safety and environmental (HSE) [1]. The data on the distribution of hydrodynamic forces resulting from the interaction between waves and ships will then be utilized as a reference for the optimization of the vessel's hull form and structural design [2]. The single-to-twin after ship hull (STASH) is one of the radical hull designs. Radical hull refers to unique designs which are formed from the existing design combinations or special design that occupied for a certain mission requirement [3]. This hull form hoped to have the advantages of both multi-hull ships and monohulls, as her form was the combination of them both. One of the disadvantages of multi-hull is her incapability to withstand waves in high seas due to her bad damping moment. Hence, this type of vessel normally only utilizes around the littoral areas [4] [5]. The lack of damping in multi-hull caused by her small amount of wet-surface area which leads to smaller surface tension compared to monohulls [6].

Although there are still rare applications and research regarding STASH, one passenger/ro-ro ship which operated in Indonesia have been applying this hull type in her design. And because of this situation, it is interesting to conduct further study about this hull design and performance, especially seakeeping. Besides that, the hydrodynamic forces which act along the ship hull during operation also need to be learned. The distribution of this force plays significant role in how the ship will respond to different sea conditions (wave number, heights, frequencies, and period) [7] [2]. The hydrodynamic forces are represented in the fluctuation of both global and sectional hydrodynamic coefficients which consist of added mass, added inertia, damping, wave excitation, stiffness, Froud-Kyrlov wave excitation, and diffraction wave excitation [8]. When the vessel operates at several significant wave heights, the hull form is one of the important elements in her seaworthiness adjustment due to the existence of hydrodynamic forces difference as the hull form differs, especially the part which interacting with water [9] [10].

Looking at the design, STASH consists of monohull-like shape at the fore part and multi-hull/catamaran-like shape at the rear. The additional hull part which fills the gap between the demi-hulls can be varied along the ship length that creates different hydrodynamic force distributions and response. In this paper the comparison of hydrodynamic forces of the STASH and Multi-hull geometry is investigated by considering the variation of the additional body along the lateral beam and how does it affect the seakeeping performance.

2. Nomenclature

$Y; \dot{Y}; \ddot{Y}$	Vectors of body position, velocity and acceleration, respectively
M	Mass matrix of the system
A_∞	Infinite added mass matrix
F_{exc}	Excitation forces vector
K_{rad}	Impulse response matrix for the radiation
C_H	Hydrostatic stiffness matrix
F_{ext}	External forces on the system imposed by the power take-off equipment and/or the mooring system
$S_w(t)$	The exact wetted surface
S_{wp} (t)	The instantaneous water plane area
x,y,z	Point on S_{wp} (t)
x_0, y_0, z_0	The coordinates of the body's origin (equal to 0,0,0 at rest)
x_g, y_g, z_g	The gravity center coordinates
x_b, y_b, z_b	The buoyancy center coordinates
C_{33} (t)	Heave modes of motion
C_{34} (t)	Surge modes of motion
C_{35} (t) = C_{53} (t)	Pitch modes of motion
C_{45} (t)	Yaw modes of motion
C_{46} (t)	Sway modes of motion
C_{55} (t)	Roll modes of motion
$S_{w,i}(t)$	The surface of i^{th} panel
x_i, z_i	The coordinates of the center of i^{th} panel
p_i	Pressure field of the incident wave
$\emptyset_0$	Incident wave potential
Re	Reynolds number
p	Pressure
T_w	Wave period
f_w	Wave frequency
Z	Simple harmonic motion
ζ_0	Wave phase difference
ω_w	Wave circular frequency
ρ	Fluid density
k	Wave number
F_{wave}	Wave force
∇ or $\forall(t)$	Volume of displacement
A_{ij}	Stiffness matrix
F_D	Diffraction force
F_{exc}	Excitation force
$\lambda = L_w$	Wavelength
F_{FK}	Froude-krylov force
$S_w(\omega_i)$	Spectrum
A_i	Amplitude i^{th} wave

3. Method

In this study, the work started with understanding the water area characteristics and preparing its mathematical model. Besides that, 3D models of several variations of STASH and a catamaran as comparison were made and being

simulated using Maxsurf Motions with designated water area conditions according to the collected data from BMKG (Meteorological, Climatological, and Geophysical Agency) which stated the three different variations of sea state in Indonesia (slight sea (0.5 m – 1.25 m); moderate sea (1.25 m – 2.5 m); and rough sea (2.5 m – 4.0 m)) [11]. To ease the research procedure the peak of wave height in each sea-state was taken as the water area data. Hence, the phase difference (ζ_0) for every sea state may be formulated as follows according to [2],

$$\zeta_0 = \zeta_a \cos\left[\frac{\pi}{2} - (kx - \omega_t)\right] \quad (1)$$

Where the wave number (k) and wave circular frequency can be written as,

$$k = \frac{2}{L_w} \quad (2)$$

$$\omega_t = 2\pi f \quad (3)$$

Single-to-twin-after ship hull (STASH) is characterized by the addition of hull between the lateral beam which is designed extending from fore peak towards the after peak with limited span and creates a monohull-catamaran hybrid look that can be illustrated as follows,

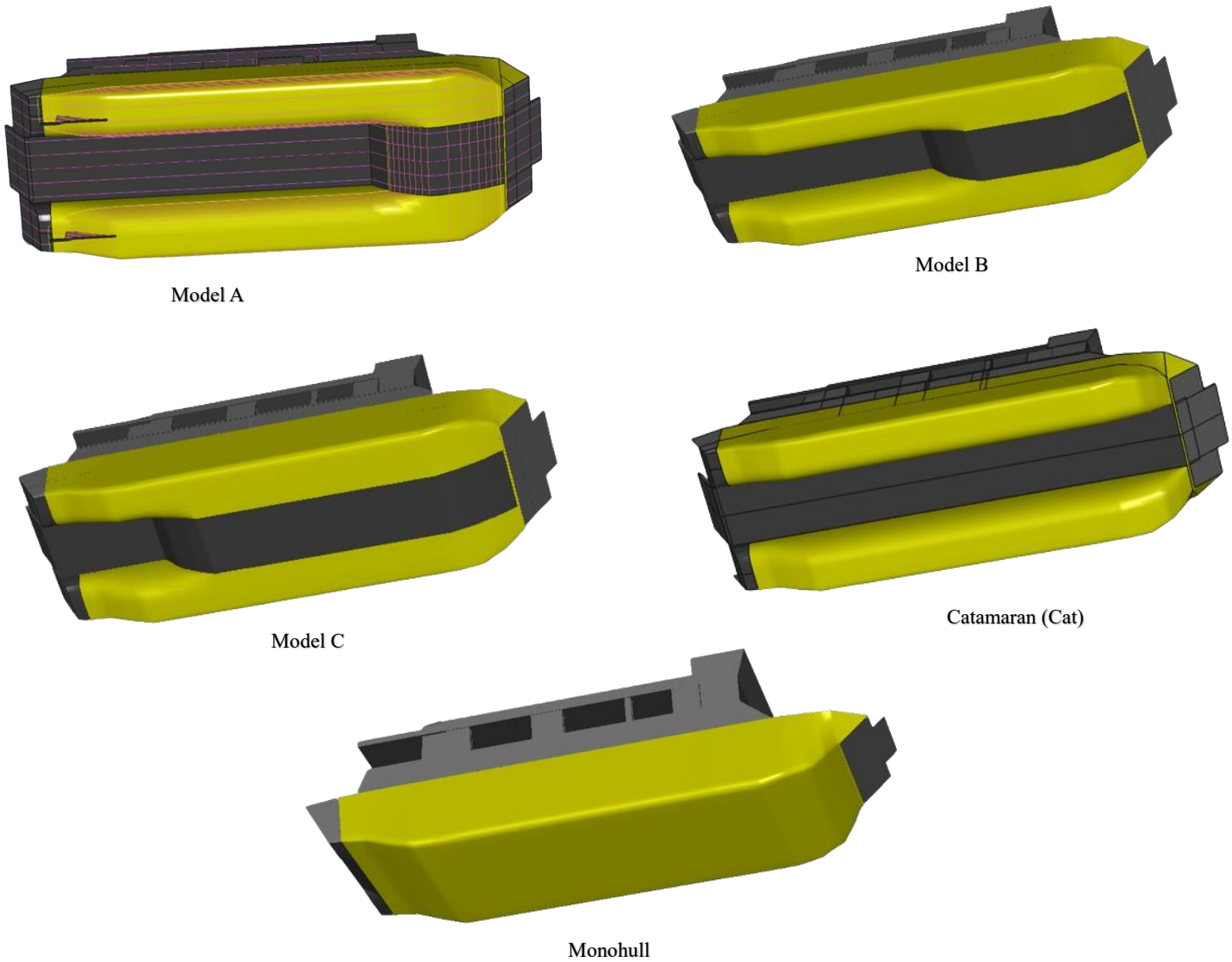

Figure 1. Single-to-twin after ship hull (model A, B, C, catamaran, and monohull).

In the research, the design of vessels is varied to create comparison. The variation limited to the extension rate of the additional hull between demi hulls, i.e. 0.25L, 0.5L, 0.85L and 1L (catamaran), block coefficients (Cb) and ship displacement as the wetted surface area (WSA) varied. The principal dimensions of the models, which include length

(L), breadth (B), depth (D) and draft (T) were taken from the original vessel which had been operating. The attempt to take the principal dimensions from an existing vessel is to ensure that the data and the case are readily available in real condition although the outcome might be theoretical. The principal dimension can be written as follows,

Table 1. Ship principal dimensions.

Items	Value (m)
Length over all (LOA)	47.90
Length between perpendiculars (LBP)	39.61
Breadth moulded (Bmld)	15.00
Depth moulded (Dmld)	3.500
draft (T)	1.890

The study utilizes Joint North Sea wave (JONSWAP) spectra for wave spectrum calculations due to its non-linearity and the ability to represent the wave-to-wave interactions in various sea conditions. The spectra can be expressed through mathematical model which states [12],

$$S_j(\omega) = \frac{\alpha g^2}{\omega^5} exp\left[-\frac{5}{4}\left(\frac{\omega_p}{\omega}\right)^4\right]\gamma^r \tag{4}$$

On the other hand, Froude-Krylov force which may be obtained using the incident wave velocity potential and defined as the force acting on the body from an undisturbed incident wave [13] [14]. Froude-Krylov force also expressed the contribution of wave diffraction, excitation and external force and how these variables may affect the hydrostatic damping of the vessel during encountering waves [15]. In general, Froude-Krylov force can be written as follows,

$$F_{FK.j} = \iint_{S_2(t)} p_i n_j \; dS \tag{5}$$

Where in nonlinear form can be expressed as,

$$F_{FK} = -\sum_{i=1}^{N} p_i n_j s_{w,i}(t) \quad \text{j = 1,2,3} \tag{6}$$

Considering the sea condition, six different motions of the vessel are assumed to occur continuously and simultaneously. Thus, each function resulting from a unit motion in j^{th} direction of a body floating in quiescent fluid. The total potential is a linear superposition of the incident, diffraction and radiation potentials, which can be written as follows,

$$\emptyset = (\emptyset_I + \emptyset_D + \emptyset_R)e^{i\omega t} \tag{7}$$

For the Froude-Krylov excitation force, each hull type has its own method of approach with different assumptions and variables. In the case of STASH, the hull which is located between the lateral beam (illustrated in Figure 1) assumed to have a similar work like an additional pontoon when encountering waves. Hence, a few basic assumptions can be made: $(b/\lambda \ll 1)$; $(B/\lambda \sim 1)$; $(a < b)$ and $(b \sim T)$. These assumptions come from the hull-wave force distribution in x-direction which occurs while the ship is operating. Thus, in the case of multi-hull vessel the Froude-Krylov force can be written as,

$$F_x^{FK} \simeq \rho bT\dot{u}(-a\omega^2)\{sin(\omega t + kB/2) + sin(\omega t - kB/2)\} \tag{8}$$

Governing the same assumption with multihull vessel, the Froude-Krylov force of STASH can be written as follows for B>>b using $g = \omega^2/k$,

$$F_x^{FK} \simeq -2\rho a\omega^2 \; sin(\omega t)\{bT \; cos(kB/2) + \delta/2 \; sin(kB/2)\} \tag{9}$$

with the adjustment to the force of the additional hull which can be defined as,

$$\delta F_x^{FK} = -2\rho ga \; sin(\omega t) \; sin\left(\frac{k}{2}(B-b)\right) \tag{10}$$

In terms of simulation, this study utilizes Maxsurf Motions to simulate the seakeeping performance of the vessel, as well as the hydrodynamic forces. The motions program streamlines seakeeping performance predictions for Maxsurf

designs, empowering designers with swift insights. It directly imports hull geometry from Maxsurf NURB surface models, eliminating the need for additional preparations. Through a user-friendly graphical interface, it presents data graphically and in tabular form, automatically updating as the analysis progresses. Upon loading a Maxsurf design, users specify analysis parameters like wave spectrum and vessel speed [16]. In the process of simulation using Maxsurf Motion, Strip theory method was used. Strip theory may be written as,

$$\frac{B}{L}, \frac{T}{L} = O(\varepsilon), \qquad \varepsilon \ll 1 \tag{11}$$

Strip theory with head seas approximation was utilized during the simulation to estimate the Froude-Krylov force variables in the simulation. Strip theory is a popular approximation of the 3D Neumann-Kelvin formulation used to predict ship motions in waves. It divides the hull of the ship into longitudinal strips and considers each strip as an independent entity subjected to wave-induced forces and moments [17] [18]. To ease the calculation process, the vessels assumed to be in an even keel condition and simulated in three different wave characteristics (1,25 m; 2.5 m; 4 m) [11]. With the assistance of head seas approximation, the assumptions of the vessel condition can be simplified and speed up the calculations to some degree. This method is exactly valid in head seas can be applied with reasonable accuracy up to approximately 20^o either side of head seas, i.e. 160^o < μ < 200^o [19] [20]. Besides that, other wave variables such as headings (θ), number of waves (k), number of frequencies, and water density were also estimated. Three wave headings were taken to be representative of head sea (3.14 rad), beam sea (1.57 rad) and following sea (0 rad).

To understand the hydrodynamic distribution, the equation of a dynamic motion based on the linear theory in a time domain is governed in the calculation [10]. The phenomena can be formulated as,

$$[M + M_{add}(\infty)]\ddot{x}(t) + \left[C_{hydro} + K_{mooring}\right]x(t) = F_{wave}(t) + F_{nonlinear_{drag}}(t) + F_{convolution}(t) \tag{12}$$

since the models were conditioned to be advancing forward and without being moored, the $K_{mooring}$ then can be assumed equals to zero. Thus, the formulae may be simplified,

$$(M + A\infty)\ddot{x}(t) = F_{FK}(t) + F_D(t) - \int_0^t k_{rad}(t-\tau)\,\dot{y}(\tau)d\tau - C_{hydro}y(t) \tag{13}$$

Furthermore, to measure the new vessels capability while cruising and encountering waves, the simulation data then compares to another clustered hull, in this case catamaran and monohull considering their close similarities in shape. Catamaran is a type of boat equipped with a twin hull which allows the vessel to have a larger space on board due to the existence of lateral beam which then makes the vessel become wider, while monohull is a common hull type which utilized by most boats ever built and contains a single hull. Besides that, this vessel is also known for its low draft which makes her suitable for cruising in a shallower water area [21] [22].

During the simulation of catamaran, the vessel was designed with the same ship principal dimensions as in Table 1. Moreover, the catamaran was also conditioned in the same water area as the other specimens to calibrate the parameter. Thus, the data may be collected for further analysis and comparison. In the case of catamaran, the Froude-Krylov force equation has a slightly different expression due to her different hull form [23] [24]. Governing the same assumption with the previous formulation in STASH, the Froude-Krylov Force of the catamaran can be written as follows,

$$F_x^{FK} \simeq \rho bT(-a\omega^2)\{sin\,(\omega t + KB/2) + sin(\omega t - KB/2)\} \tag{14}$$

In the case of monohull, a different approach must be taken (both vertically and horizontally) to express the phenomenon due to its different hull form. Since the monohull consists of better restoring moments during encountering waves, restoring coefficients such as C_{33} (heave restoring coefficient) and C_{55} (roll restoring coefficient) are integrated in the formulae [10] [25]. The integration of C_{33} also requires the consideration of free surface elevation $\eta(x,t)$, which can be expressed as follows,

$$C_{33} = \rho g \sum_{i=1}^{N}\left(n_{3,i}S_{\omega,i}(t)\right) \tag{15}$$

$$\eta(x,t) = Re\{ae^{i(\omega t - kx)}\} \tag{16}$$

$$C_{55} = \rho g \sum_{i=1}^{N}\left(\left(x_{1,i}(t) - x_{0_1}(t)\right)^2 n_{3,i}S_{w,i}(t)\right) + \rho g \forall(t)x_{b_3}(t) - mgx_{g_3}(t) \tag{17}$$

$$C_{35} = -\rho g \sum_{i=1}^{N} \left(\left(x_{2,i}(t) - x_{0_2}(t) \right)^2 n_{3,i} \, S_{\omega,i}(t) \right) + \rho g \forall(t)_{x_{b3}}(t) - mg x_{g3}(t) \quad (18)$$

The overall integration of these three variables then provides vertical and horizontal Froude-Krylov force formulae for single hull (monohull) which then being composed together and brings the final expression of the final formulae which expressed as follows,

$$F_x(t) \simeq Re\left\{ \rho TB \, \dot{u}(x = 0, z = 0, t) + \frac{2\rho}{k^2} e^{-kT} sin(kB/2) \dot{w}(0,0,t) \right\} \quad (19)$$

Moreover, this work was conducted on a computer with the process mainly using the processor, while the GPU has already used ray tracing technology. The specification of the computer can be mentioned as follows:

Processor : 11th Gen Intel® Core™ i5-11400H @ 2.70GHz (12 CPUs), ~2.7GHz
Memory : 16384MB RAM
BIOS : E16R6IMS.113
GPU : NVIDIA GeForce RTX 3050
DAC Type : Integrated RAMDAC
Display Memory : 3965 MB

4. Results and Discussion

The investigation of hydrodynamic force of single-to-twin after ship hull (STASH), catamaran and monohull have done successfully. The method perfectly calculates the variables which represent the distribution of the forces along the ship body and how well the vessel reacts to the force that she encountered in several speed and wave height variations. In the vast expanse of the ocean, a ship's journey is an intricate dance with the elements, governed by the complex motions that define its voyage. These motions, influenced by the relentless forces of wind, waves, and currents, dictate the ship's stability, safety, and comfort. Heave, pitch and roll, the primary motions, are caused by the interplay of external forces acting on the vessel, creating a rhythmic oscillation that sailors must constantly navigate.

4.1. Ship Motions

Various ship motions at sea are affected by several factors including hull form, waves, currents, weather, velocity (whether it's the ships or the waves or other phenomenon), frequencies, hull displacement, etc. Looking at the ship response to waves which coming from different angles of attacks, namely head sea (3,14 rad), beam sea (1,57 rad) and following sea (0 rad) RAO in various encountered frequencies giving varied results due to the existence of different hull models.

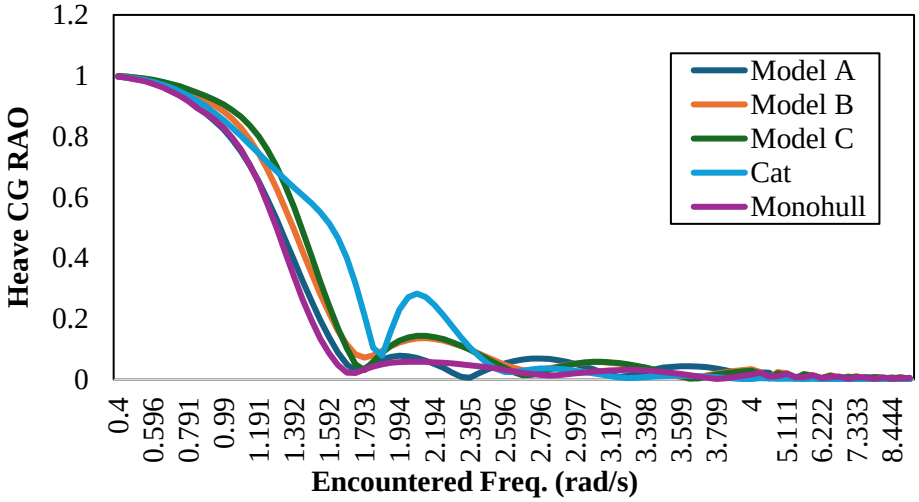

Figure 2. Heave RAO model a, b, c, catamaran, and monohull (head sea) in 5 knots.

While encountering waves, cruising speed is one of the factors which affect the ship response. Hence, velocity difference determines whether the total force received by hull that then caused those motion intensity variants. On the other hand, hull form also being another factor due to its correlation to the total displacement. As seen in Figure 2, which represents the behavior of each hull model during head sea with gradually increased frequencies in 5 knots,

Catamaran (Cat) is more sensitive to heave compared to other hull forms. Catamaran tends to have relatively small total displacement due to her smaller amount of wetted-surface area. This small displacement means the ship has lighter weight compared to the other models, which then results in a higher response to wave force even when cruising at lower velocity. This sensitive behavior while encountering waves is also shown by the STASH model which may be seen in all RAO graphs in every angle of attacks (head sea, beam sea and following sea).

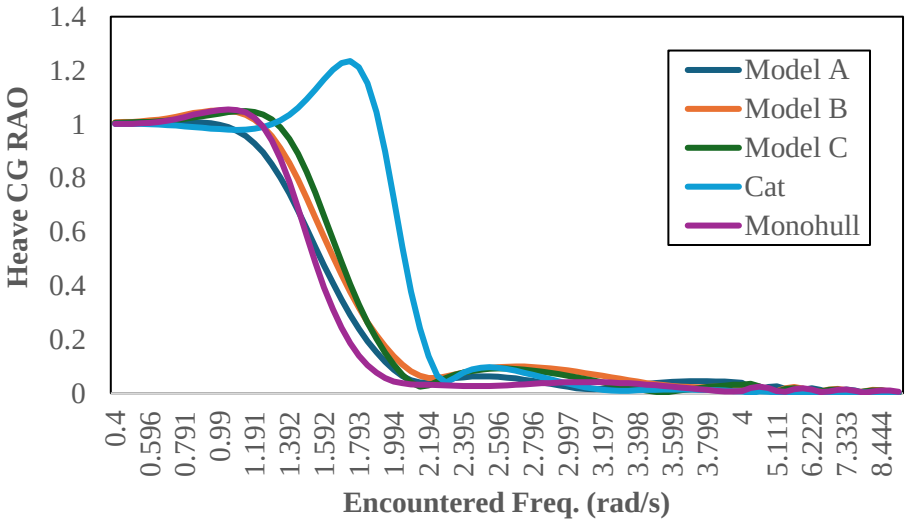

Figure 3. Heave RAO model a, b, c, catamaran, and monohull (head Sea) in 10 knots.

The right amount of wetted-surface area (WSA) is important to sustain both buoyancy and ship responses. A higher amount of WSA allows a higher amount waterplane area (WPA) to be owned in most ship hull forms. Bigger WPA enables the ship to grasp a bigger amount of surface tension of the water. The surface tension plays a role in gripping the hull to stay on the water surface. Besides that, bigger WSA might also mean better buoyancy as it allows the vessel to have more rooms where air can be stored to keep the vessel upward. As may be seen in Figure 3, the overall heave motion RAO of each model increased due to the higher velocity (10 knots). STASH models are also experiencing the same phenomenon. Those which have the least amount of WSA (model A) have the highest sensitivity of motion sensitivity. The increase in heave motion of catamaran at 10 knots speed is up to 75% compared to the 5 knots velocity, while STASH models and monohull stay in the relatively same motion intensity. There are a bit increases in earlier frequencies, such as 0,99 rad/s to 1,291 rad/s in 10 knots and 1,105 rad/s to 1,539 rad/s in 15 knots (see Figure 4) due to the increase in velocity and shorter wavelength which make shorter travel distances between wave crests and troughs. At 10 knots, the peak heave RAO for the catamaran occurs around 1,983 rad/s, which is slightly lower than at 15 knots (see Figure 4), reflecting the influence of speed on resonant frequencies. On the other hand, twin hulls can cause wake interference due to the existence of gap between demi hulls which may accumulate wave force in that void and contribute to pushing the vessel upward.

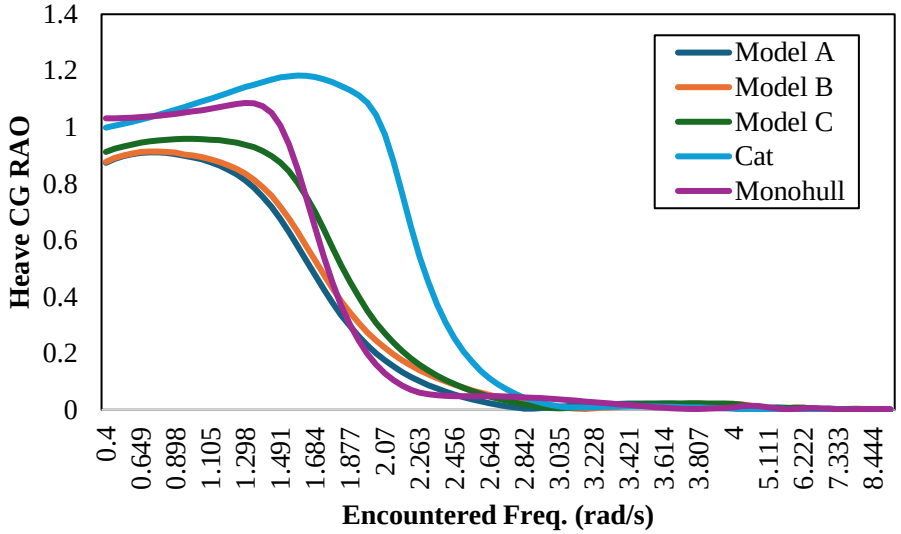

Figure 4. Heave RAO model a, b, c, catamaran, and monohull (head sea) in 15 knots.

The heave RAO values for all vessel types decline steadily beyond the peak frequency, with the catamaran again showing a sharper decline. This suggests that while the catamaran is sensitive to resonant frequencies, it also has good damping characteristics to reduce vertical motions effectively. In contrast, STASH (model A, B, C) and monohull still have lower damping characteristics. The motion sensitivity, however, is not as high as the catamaran although the motion sensitivity is better than catamaran.

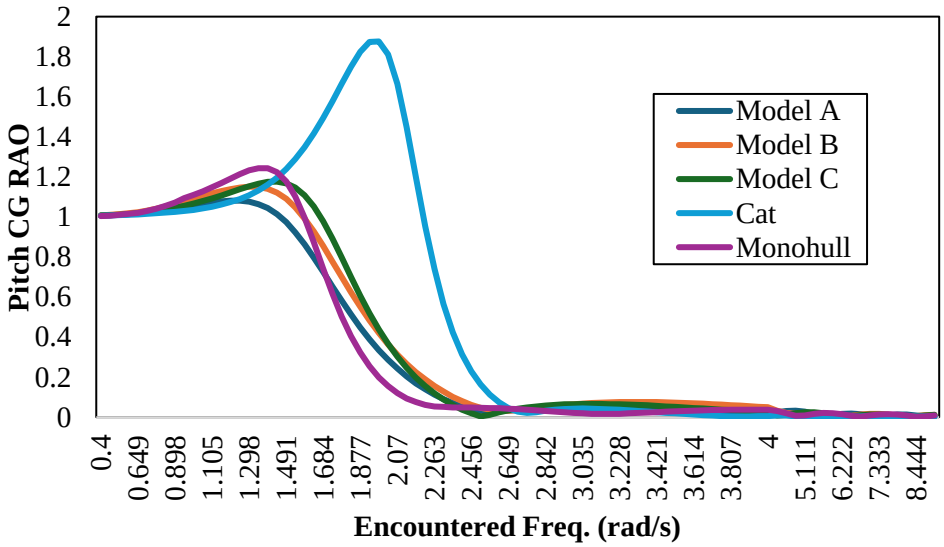

Figure 5. Pitch RAO model a, b, c, catamaran, and monohull (head sea) in 15 knots.

In the case of pitch motion, similarly shaped curves motion pattern can be seen in the RAO graph represented in Figure 5. Monohull and Catamaran, however, show a more dramatic change in response to waves due to their hull form. From the graph, the impact of hull form and displacement still significantly affects the ship motion, although both catamaran and monohull show a significant response (in heave and pitch), there is a different type of response that we can highlight in their behavior while receiving the wave force. In Figure 5, 6 and 7, the monohull shows response in shorter range of frequency which indicates the wave needs to have a bigger volume and shorter length to move the vessel. The bigger volume may create deeper trough and higher crest, which makes the more extreme gap between these wave parts and make a significant difference of drafts in the fore area and aft area, while lower frequency tends to make the wave number decrease. Due to these two factors, the rate of response to wave amplitude or RAO (in this case pitch) may grow higher. In the case of monohull, this type of vessel needs a bigger volume of waves and longer wavelength to move is because of her weight which significantly bigger compared to other forms (STASH and

catamaran). Thus, a bigger force is needed to uplift that big amount of displacement with, of course, not forgetting the influence of surface tension.

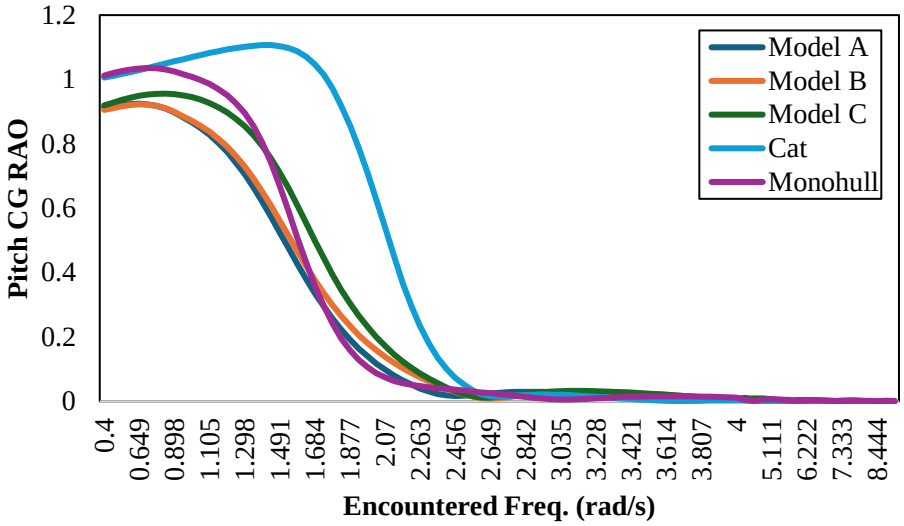

Figure 6. Pitch RAO model a, b, c, catamaran, and monohull (head sea) in 10 knots.

While STASH shows relatively stable response (in pitch) compared to the other conventional hull form, among the three models model A shows the least pitch response followed by model B and model C (see Figure 5,6 and 7). The result of the simulation indicates that there are no changes in what model did have the least pitch motion. In lower speed, such as 5 knots, however, STASH also shows worse damping performance due to their lower motion momentum since in lower speed the vessel – wave interaction is also lower. Hence, the force delivery from the wave to the hull is also slower.

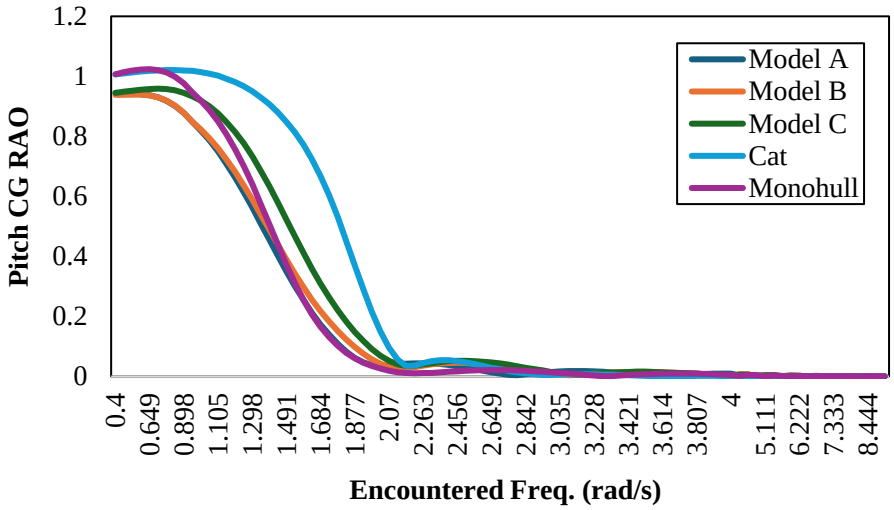

Figure 7. Pitch RAO model a, b, c, catamaran, and monohull (head sea) in 5 knots.

During the simulation of the vessel models in Head Sea, there are no roll motions which arise in the process. This phenomenon occurs due to the angle of wave approach which only comes from 3,14 rad and makes the angle in line with the vessel. Such sea conditions shall not trigger any rolling motion while there are some wave-vessel interactions. The possibility of triggering roll motion in head sea shall increase if the wave incidence angle was made away a bit or significantly from the 3,14 rad which are not conducted during the research due to non-necessity and infectivity as the data which might appear shall be too much to handle. Besides that, big amounts of data shall take a

longer period to be processed, while roll motion phenomena have already been analyzed and represented in Beam Sea data.

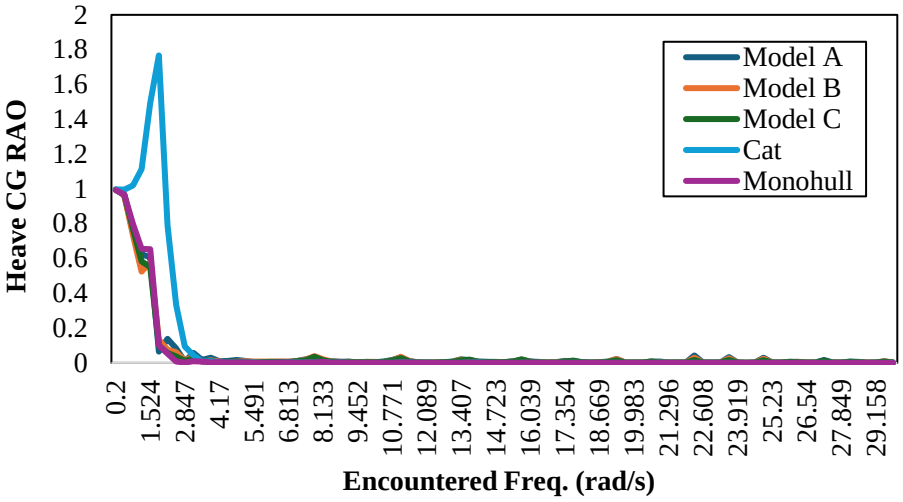

Figure 8. Heave RAO model a, b, c, catamaran, and monohull (beam sea) in 5 knots.

In Beam Sea, three different motions (heave, pitch and roll) occur during the simulation. While encountering the waves from 1,57 rad, Catamaran still showing the biggest heaving response rate compared to the other models. The same reason still applies to this phenomenon, which is the same as in the Head Sea conditions. In their gradual decrease in motion rate, from the lowest value around 3,178 rad/s to 29,812 rad/s frequency, STASH still experienced fluctuation in heave motion rate. Compared to monohull and catamaran, STASH models are more responsive in higher frequency which tends to be more silenced. This phenomenon occurs due to the STASH hull form which is the combination of monohull and catamaran. This hull form creates unstable wake form while going through the ship body, especially if the wave comes from the sides (Beam Sea) whether it is at port side or starboard side. This different wake form then leads to the different wave force which acts around the fore parts and after parts of the hull. As can be seen in Figure 1, the catamaran after body consists of twin hulls and a niche which being the connector of the ship body as the monohull begins to convert into catamaran. These parts shall trigger more intense turbulence and fluid flow interference if the angle of wave approaches subjected from the side. Those phenomena gave rise a little to instability of motions, even when damping has already been induced to the vessel as the encountered frequency increases.

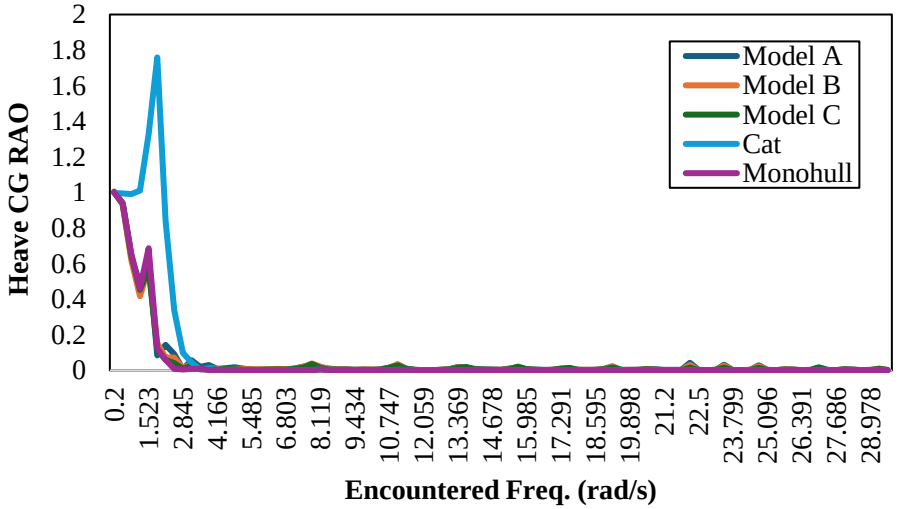

Figure 9. Heave RAO model a, b, c, catamaran, and monohull (beam Sea) in 10 knots.

The same fluctuation of motions after induced damping also appears in the relatively higher velocity, such as 10 knots and 15 knots. Due to higher speed, the peak of RAO encountered frequency of 1,192 rad/s showing different

value compared to the relatively lower speed, 5 knots. Besides due to the increase of velocity which causing the shorter travel period for the waves, this increase of response occurred because of the hull form. Apart from the fore and the after parts of the ship, the side shell consists of less curves. Thus, the fluid never flows smoothly which then leads to more wave slamming. This phenomenon not only contributes to higher heave motion, but also roll motion (see Figure 11, 12, and 13) due to the wave transport and force which now acts like pushing the ship rather than uplifting her. Moreover, the twin hull-after part also being another cause for this fluctuation and higher motion rates. The existence of twin hulls in the after body generates different wave patterns compared to the monohull part in the fore body. Due to its short distance gap under the lateral beam, the ever-changing wave pattern can be more intense as the speed increases as well as the fluid flow interference which also contributed to a more fluctuating excitation (or hydrodynamic force (see Figure 23, 24, and 25).

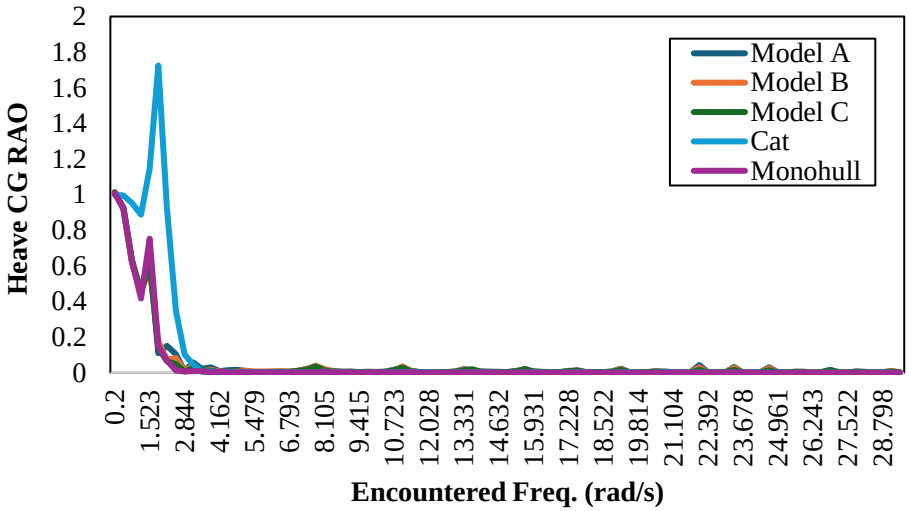

Figure 10. Heave RAO model a, b, c, catamaran, and monohull (beam sea) in 15 knots.

Although there is a fluctuating response to amplitude of heave motion in Beam Sea conditions, the principle where the ship may cruise much smoother at higher speed still applies. Despite all the phenomena which have been discovered and discussed in the previous paragraphs, STASH in particular, showing unique characteristics and the hull design quite impactful in decreasing the heave and pitch motions in various speeds compared to conventional monohull and catamaran. In contrast, several configurations of STASH, such as model A and C, show a quite worse performance in roll motion compared to monohull and catamaran in all velocity variants. This occurrence influenced by non-others than the hull form itself. Compared to catamaran, STASH relatively have more turbulence associated with the instability of the fluid flow and wave force deliverance due to the existence of twin hulls and monohull combination. The intense roll motions in model A and model C are influenced by those factors and these two models, however, do have different cases. In the case of model A, due to the long span of lateral beam (from after body), which may be called tunnel, the total displacement of the vessel is close to catamaran. However, model A consists of an additional pontoon-shaped part around the fore peak area (see Figure 1) which creates a difference in wave transport. Moreover, this additional part only has a short longitudinal span, so that there is a relatively extreme curve in the monohull-to-catamaran transition which means, a fast-flowing fluid which creates turbulence also occurred in that area. These phenomena finally accumulated with the raw wave force and became another contributor to the motion intensity of the vessel model A. Contrary with model A, model C shaped from a longer span of additional pontoon-shaped part (see Figure 1) which make the monohull part is a lot more dominant compared to the twin hulls. This condition creates less turbulence due to a fast-flowing fluid compared to model A or model B and catamaran. Besides that, this hull triggers more resting fluid conditions which consist of the same amount of hydrodynamic force. However, this composition also allows the wave force to be delivered to full potential since there is only a small gap along the lateral beam. Thus, there is almost nothing that may split the wave before being transported away from the hull. This full loaded force from the wave is the thing that pushes the vessel to roll.

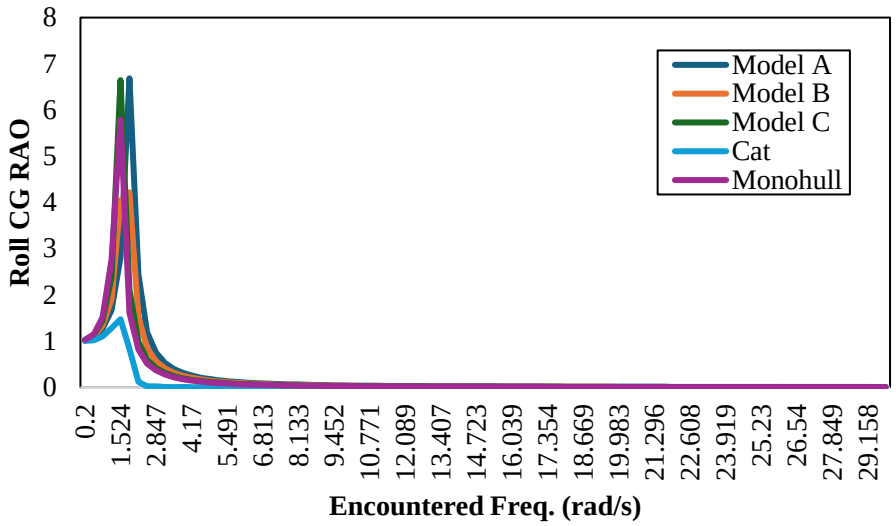

Figure 11. Roll RAO model a, b, c, catamaran, and monohull (beam sea) in 5 knots.

The graph 11, 12, and 13 illustrate the encounter frequency responses for five different models: Model A, Model B, Model C, Catamaran, and Monohull, the encounter frequency on the x-axis is plotted against a response metric on the y-axis, revealing distinct patterns in how each model behaves under different conditions. All models exhibit a significant peak in response around 1-2 rad/s. This peak is most pronounced in Models A, B, and C, which show slightly higher maxima compared to the Monohull and Catamaran models. The Catamaran model, however, displays a noticeable dip immediately following its peak, distinguishing it from the other models. In contrast, the Monohull model presents a smoother decline post-peak, indicating a more gradual decrease in response. Beyond the peak, the response curves for all models drop sharply and converge towards zero as the frequency encountered increases. This rapid decline suggests that higher frequencies have less impact on the models' responses. Despite the overall similar trend, subtle differences are observed: the Catamaran model's post-peak dip is more prominent, whereas the Monohull model maintains a relatively even and stable response curve. These distinctions point to variations in how each model manages dynamic loading and frequency changes, with the Monohull model potentially offering more consistent performance across a broader range of frequencies.

These graphs collectively provide valuable insights into the dynamic behaviors of different ship design models. The pronounced peaks around 1-2 rad/s indicate a common resonance frequency range where all models are most responsive. However, the differences in peak heights and post-peak behaviors underscore the unique characteristics of each design. Models A, B, and C, with their higher peaks, might be more sensitive to specific dynamic loads, while the Catamaran model's distinct dip could imply a unique damping characteristic. The Monohull model's smoother curve suggests a potentially more stable and reliable performance across varying conditions. These observations can inform decisions in naval architecture, helping to select the most appropriate model based on the desired performance criteria in dynamic environments.

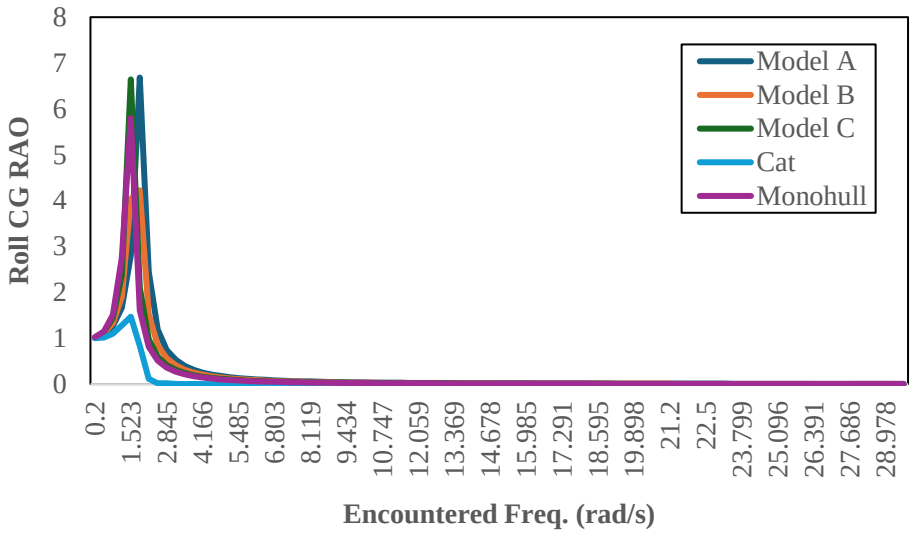

Figure 12. Roll RAO model a, b, c, catamaran, and monohull (beam sea) in 10 knots.

All models exhibit a prominent peak at low frequencies (around 1-2 rad/s), with Model A, B, and C showing nearly identical, slightly higher peaks than Monohull and Catamaran. Beyond these frequencies, responses sharply decline and stabilize near zero, indicating low sensitivity to high-frequency encounters. Catamaran exhibits a unique dip post-peak, while Monohull shows the smoothest curve with a gradual decrease, highlighting varied stability and resonance characteristics among the models. In those graphs, however, it shows model B STASH roll motion intensity is relatively moderate in those velocity variants. The catamaran and monohull exhibit more favorable roll performance across the frequency range, especially beyond the peak frequency, where their RAO values remain consistently lower. Models A, B, and C exhibit similar roll behaviors, which are slightly less favorable than those of the catamaran and monohull. The significant peak in roll RAO around 1.523 rad/s highlights a critical natural frequency for roll motion, emphasizing the need for understanding and mitigating roll in these vessel types. This analysis underscores the importance of considering roll RAO in vessel design and operation, particularly in beam seas, with the catamaran and monohull generally offering improved comfort and safety in such conditions. The phenomenon occurs due to the equal length between monohull and catamaran. This equality creates an equilibrium between the fully delivered force of wave in the fore body and wave interference in the after body. In this case the principle of fluid dynamics has been fulfilled where the hydrodynamic equilibrium has been reached in the term of force. Thus, the roll motion of model B is relatively low compared to model A, model C and monohull. Besides that, lower roll motion intensity leads to better comfort while cruising and encountering wave heights.

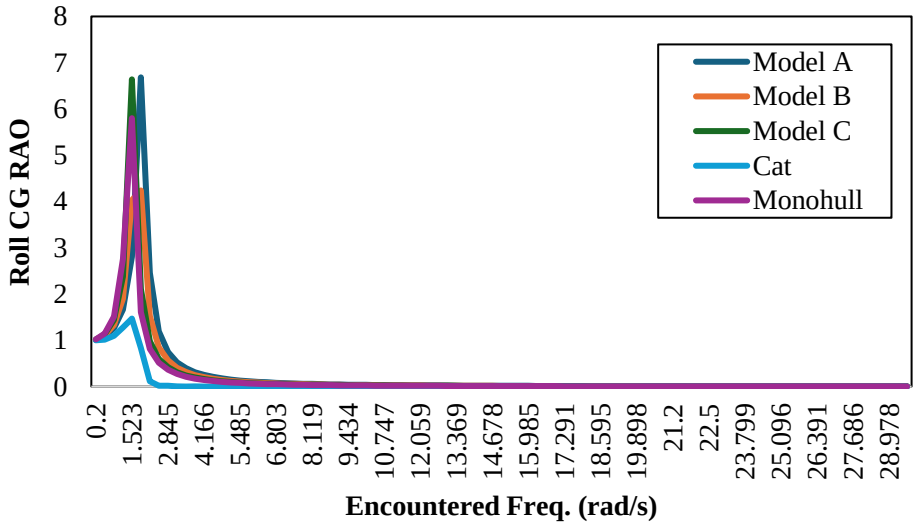

Figure 13. Roll RAO model a, b, c, catamaran, and monohull (beam sea) in 15 knots.

The provided graphs in Figures 14, 15 and 16 illustrate the pitch RAOs (Response Amplitude Operators) across various wave frequencies with a 1.57 rad angle of attack for different models: Model A, Model B, Model C, Catamaran (Cat), and Monohull. The x-axis represents the encountered frequency (rad/s), while the y-axis represents the pitch RAO, measuring how much the vessel pitches in response to wave action. Across all three graphs, we observe that Models B and Monohull consistently exhibit the highest peak RAO values in the lower frequency range, indicating greater sensitivity to low-frequency waves. This heightened response suggests that these models may experience more pronounced pitching motions, which can adversely affect stability and comfort.

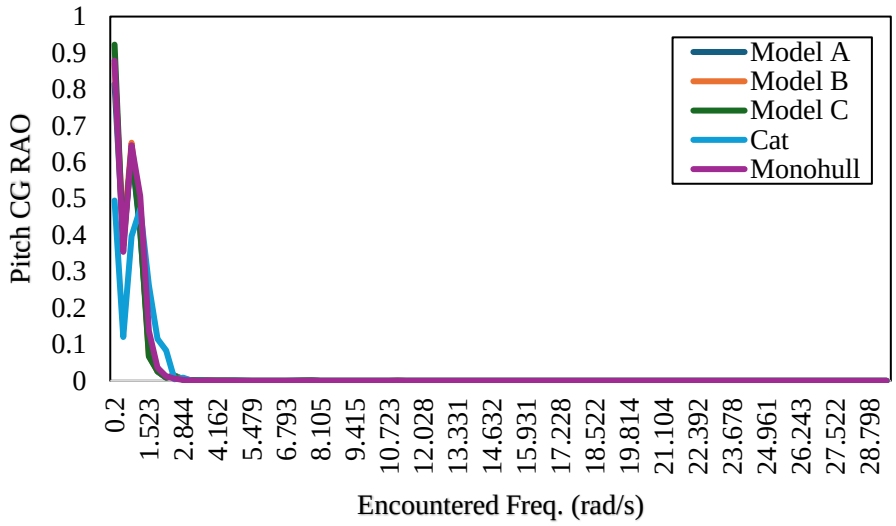

Figure 14. Pitch RAO model a, b, c, catamaran, and monohull (beam sea) in 15 knots.

Analyzing the models further, the sharp decrease in RAO values after approximately 3 rad/s is consistent across all models might be seen. This trend indicates that the pitch response diminishes significantly at higher frequencies, reflecting a common characteristic among the different designs. This pattern underscores the fact that while all models become less responsive to wave action at higher frequencies, the degree of initial sensitivity at lower frequencies varies notably between them. Models B and Monohull, demonstrating heightened pitch responses at lower frequencies, could lead to increased discomfort and potential safety concerns in rough sea conditions. In contrast, Models C and Cat, with their relatively lower peak RAO values, suggest better performance in terms of maintaining stability and minimizing pitching motion. Although it may be less significantly giving the effect of discomfort like roll motion, lower pitching motion may prevent the ship from flipping as the hull is not distancing from the water surface that often. Besides that, less pitch also means less slamming. Thus, additional force may decrease, and more structure fatigue can be avoided during the cruise which leads to further damage to the whole construction system caused by slamming the wave like what monohull may experience. The high peak of pitch motion of the monohull comes from her inability to split the wave which makes the force decrease. Although the split may create interference, the lift caused by the wave impulse may decline quite significantly.

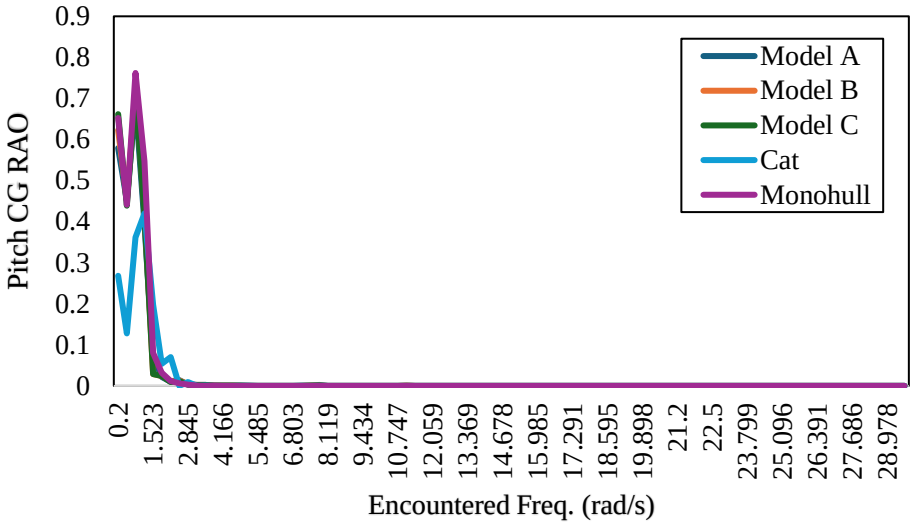

Figure 15. Pitch RAO model a, b, c, catamaran, and monohull (beam sea) in 10 knots.

The implications of these findings for seakeeping are significant. Models C and Cat emerge as superior choices, particularly in environments characterized by low-frequency waves. Their lower peak RAO values imply that these designs offer enhanced stability and comfort, which are critical for both passenger safety and operational efficiency. This enhanced performance can translate to smoother rides and reduce the risk of motion sickness, making these vessels more suitable for commercial and passenger operations. Conversely, Models B and Monohull, with their higher sensitivity to low-frequency waves, may result in less comfortable and potentially more hazardous conditions, particularly in rough seas. The consistent reduction in RAO values at higher frequencies for all models further emphasizes the advantage of selecting designs. In the selection of the models, however, the analysis of each motion should be considered, since in real deal all types of motion occur at the same time and influence the whole systems integrated in the ship differently.

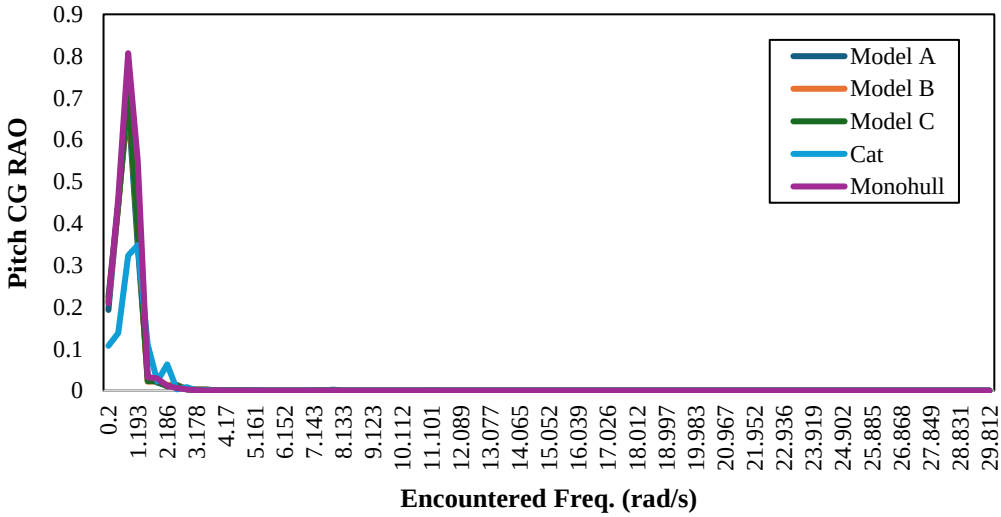

Figure 16. Pitch RAO model a, b, c, catamaran, and monohull (beam sea) in 5 knots.

Certain results also can be taken from the heave motion analysis in following sea which represents in Figure 17, 18, and 19. In the condition of following sea, as we have known, the wave force delivered from behind the ship. The following sea refers to the waves or fluids which flow from the after body to the fore body (the inverse of head sea). On the other hand, when encountering the following sea condition, the vessel models show different characteristics compared to the other angle of attacks. Every model reached their peak of motion intensity in the negative wave frequencies. Compared to other designs, catamaran, again, being the model which has the least response. However, in

this case the reason for this phenomenon is more than the ship weight distribution or displacement but more to what did the models have experienced.

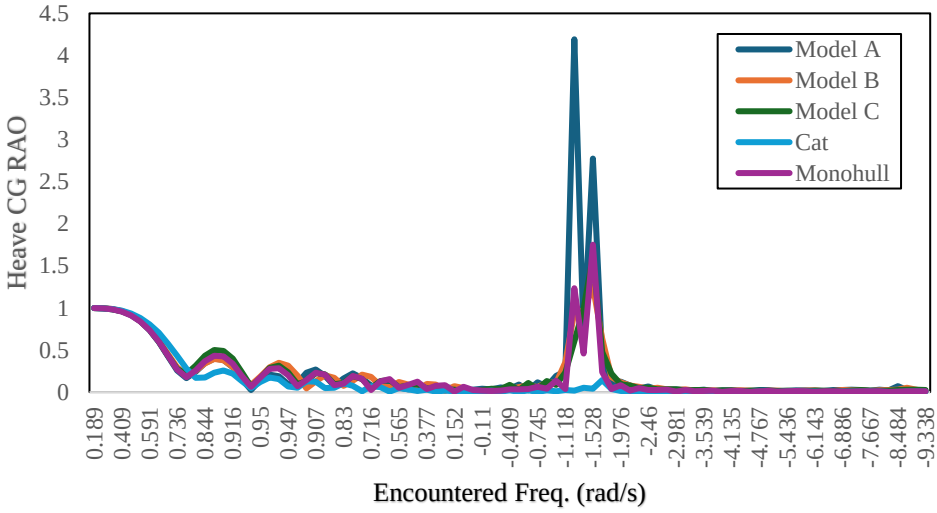

Figure 17. Heave RAO model a, b, c, catamaran, and monohull (following sea) in 5 knots.

Like what has been discussed previously, ship motion is influenced by many contributing variables. Hence, unique behaviors naturally occur based on those influencing factors. In the case of following sea, the wave force, instead of directly encountering an extremely curved surface, a relatively smooth surface was passed first. This condition tends to make the flow speed more conducive, which means there is less lift caused by the increase of fluid flow velocity. Small fluctuations, however, still occur due to larger influences of wave interference in lower speed, such as 5 knots. But on the other hand, such phenomenon supports wave building conditions which generate an accumulation and contributes to the intense ship motion in a later period. The longer the longitudinal lateral beam span (tunnel), the longer the building condition is a period to accumulate the wave force. Thus, a high intensity of motion may occur, which is also experienced by model A.

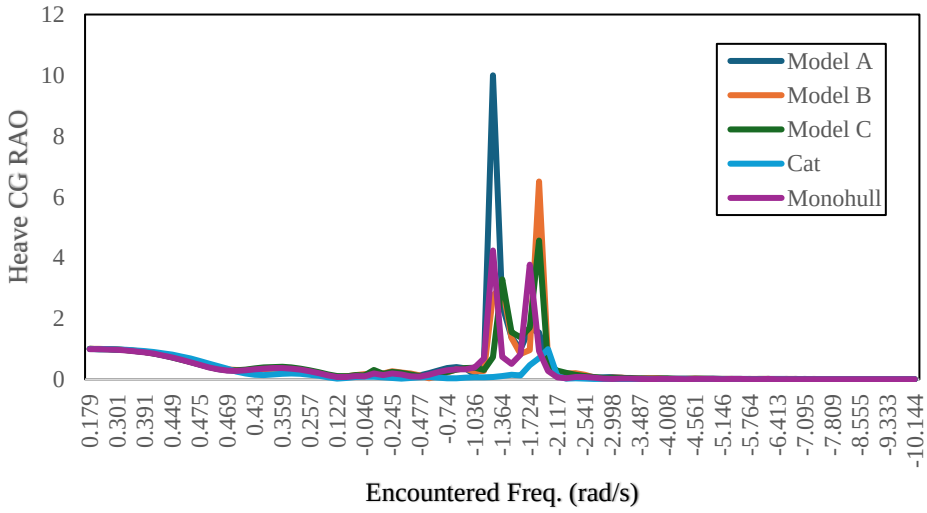

Figure 18. Heave RAO model a, b, c, catamaran, and monohull (following sea) in 10 knots.

Moreover, the following sea condition also shows an interesting thing as the ship velocity increases. As might be seen in Figure 18 and 19, the peak of motion intensity differs make the models have more than one peak. When the wave travels at a relatively higher speed, the wake generation is also faster. This leads the wave to disruptions to some extent as the velocity now is high enough to create an oscillation after the wave reached the final trace where the longitudinal tunnel ends. Those waves which oscillate then collide with the newly coming waves which then create

other accumulated forces which lifts the ship upward. Since the ship motion generated from the wave collision, meaning the energy to push the ship upwards needs a period to occur. Thus, ship motion may vary in different frequencies. Among the STASH model, in the following sea, model C generates less motion compared to the other (model A and B). This occurrence happens due to her shorter longitudinal tunnel span which prevents a further wave force building condition.

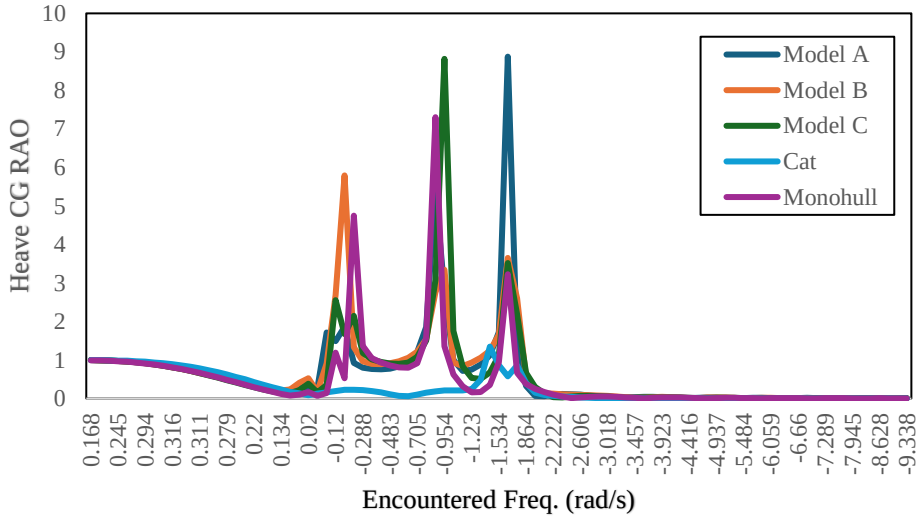

Figure 19. Heave RAO model a, b, c, catamaran, and monohull (following sea) in 15 knots.

Similarly with head sea, following sea condition did not generate roll motion when the angle of attack determined in 0 rad. For this phenomenon, the same reason as what we have in heave motion applies where the wave only goes through a track in-line with the ship cruising direction. And due to different ways of wave-to-hull force deliverance, the motion intensity of the vessel also differs. In the case of pitching motion, unique characteristics can be seen presented in Figure 20, 21, and 22. In contrast to heave motion in the following sea condition, pitch motion created a more positive damping as the speed reduced. On the other hand, building conditions also can be seen in relatively positive frequencies which also influences damping as well.

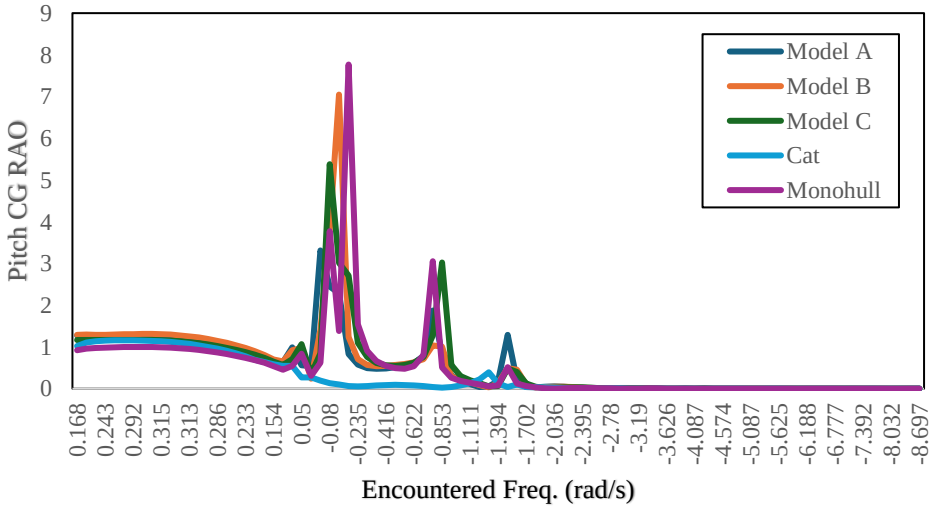

Figure 20. Pitch RAO model a, b, c, catamaran monohull (following sea) in 15 knots.

In terms of hull form, pitching in the following sea generated relatively negative frequencies, due to her monohull shape in the fore peak area. The tunnel of the twin hull still being a huge factor of reducing pitch motion, while reversed flow also generated by the monohull form in the fore peak also contributed to the accumulated wave force. Moreover, monohull generated the highest pitch motion in the higher velocity followed by model B, while model A and model C

are equal and catamaran being the least responsive. In the higher velocity encountered a larger wave number, model B having the higher motion intensity among STASH model due to her equal portion between twin hull and monohull, making the ship reach its equilibrium (where the vessel is not too light and not too heavy as well). Thus, similar characteristics with monohull appeared.

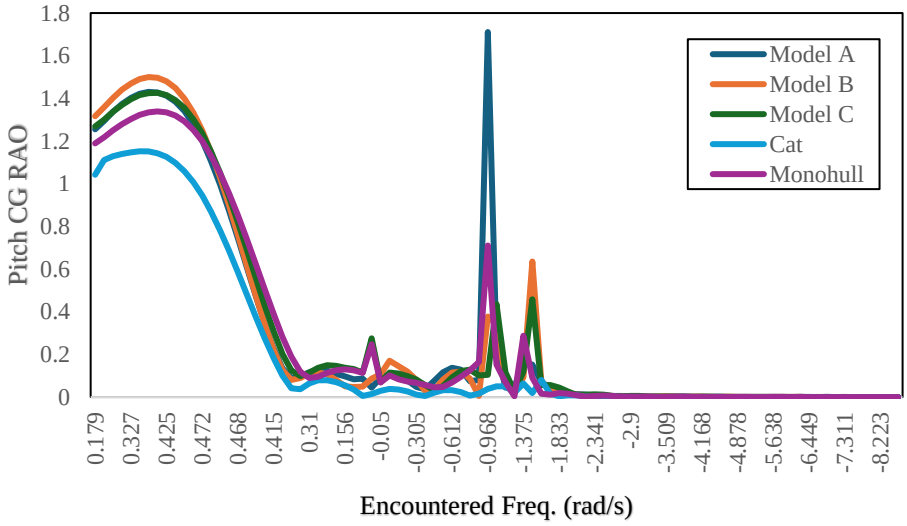

Figure 21. Pitch RAO model a, b, c, catamaran monohull (following sea) in 10 knots.

In medium speed, a more gradual pitch motion begins to dominate the fluctuation of pitch motion intensity in positive frequencies. In this condition the balanced pendulum-like phenomenon which occurs in model B like in the higher speed (15 knots) is no longer happening. This change of motion characteristics experienced by model B was because the equilibrium is no longer reached since the wave number in the lower speed is also decreased. Hence, the principal conservation of momentum in the higher velocity cannot be applied anymore. One unique thing occurred in model A which reached the highest peak of pitch motion intensity in -0,968 rad/s. As has been discussed previously, model A is the one with the lowest displacement among the STASH model. This light weight then boosts the motion intensity as it is easier for the wave force to push the vessel and generate more pitch, especially when encountering irregular waves.

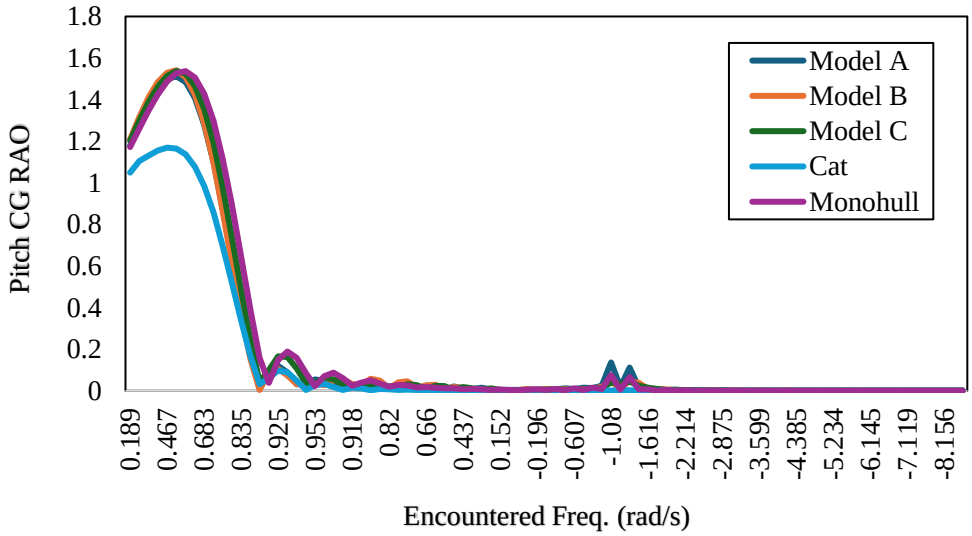

Figure 22. Pitch RAO model a, b, c, catamaran monohull (following sea) in 5 knots.

Finally, in terms of seakeeping STASH models come in various characteristics. The overall simulated ship motion results show that STASH did make different responses due to her hull form. However, compared to monohull

and catamaran, this hull design did not perform better. Several higher motion intensities still occur in several sea conditions, which means this radical shape cannot contribute significantly to decreasing ship motion.

4.2. Hydrodynamic Force

The investigation of hydrodynamic force acting along the ship body is one of the crucial things to study in the basic design stage. The fluctuation and transport of the hydrodynamic force can be analyzed and represented through Froude-Krylov force. Froude-Krylov force (NFK) is the force which is influenced by the unsteady pressure field generated from undisturbed waves, while also together with diffraction force, make up the total non-viscous forces acting on a floating body in regular waves. The distribution of the hydrodynamic force also, like motions, varies as it reliant to wave propagation along the ship body.

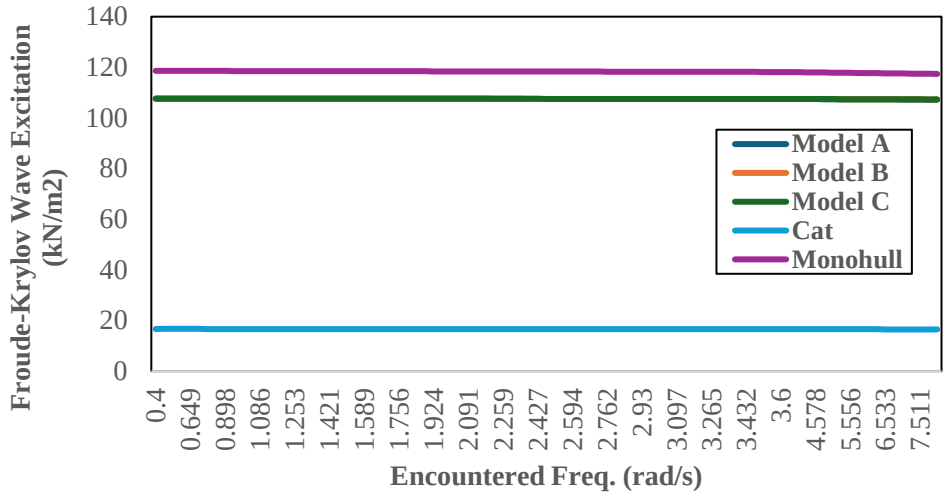

Figure 23. Froude-Krylov wave excitation (head sea) model a, b, c, catamaran, monohull in 15 knots.

The wave phase of each sea condition differs following its dispersion and propagation. In theory, the more complex the shape of the specimen, the more wave dispersion phenomena generated along the way. The term hull complexity includes curvature, material texture, and additional appendages or other systems, such as propulsion. Besides that, the Froude-Krylov excitation is acting on the body from undistributed incident wave which is influenced by wave velocity potential. In all sea conditions, fluctuation of force occurs in different encountered frequencies. Various characteristics are shown in different angles of attacks and velocity which are affected by the hull form diversity.

In the head sea (all speed variants), the highest wave excitation occurs at monohull and catamaran at the lowest. This phenomenon happened because monohull has the biggest wetted-surface area (WSA) compared to all models which being simulated. Based on the same reason, STASH models (model A, B, and C) are in the middle with model A which has the lowest value and model C the highest. Looking at the data represented in the graphs (see figure 23, 24, and 25), the amount of wave excitation on STASH hull models are close to the monohull rather than to catamaran due to their hull form and the hydrodynamic phenomena they created when simulated approximately 20 kN/m^2 in head sea. The amount of wetted-surface area (WSA) directly affected to the Froude-Krylov force since the bigger WSA, the bigger hull – fluid interaction which occurs while cruising. On the other hand, the complexity of hull design being other factor which influences the value of hydrodynamic force in general. Wake, spray, fluid flow interference, friction and other fluid dynamics occurrences are varied based on the hull design.

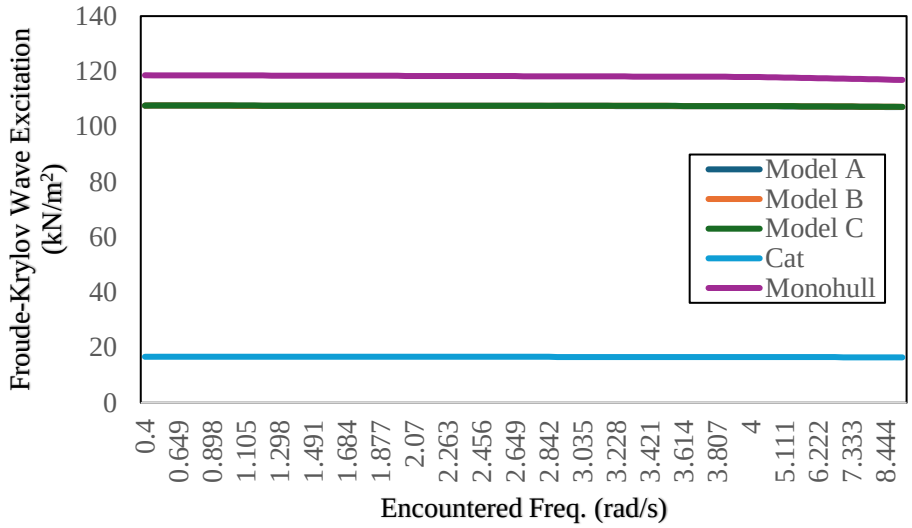

Figure 24. Froude-Krylov Wave Excitation (Head Sea) Model A, B, C, Catamaran, Monohull in 10 knots.

Overall, in head sea STASH showing quite identical trends with only minor divergence at higher frequencies indicating that those models have comparable hydrodynamic phenomena, particularly in Froude-Krylov wave excitation. On the other hand, model C, although showing similar data compared to model A and B shows a slightly steeper decline in wave excitation at higher frequencies, suggesting a marginally different effect under these conditions. Thus, model C has a more pronounced reduction in wave excitation as the frequency increases. Moreover, STASH hull designs generating more wake due to the existence of monohull-like form around the fore peak area. This transitional area from monohull to twin hull in the after peak contributes on generating this wake which combined with the fluid flow interference generated by the twin hull. Hence, more wave excitation is generated as the hull and fluid flow interacts.

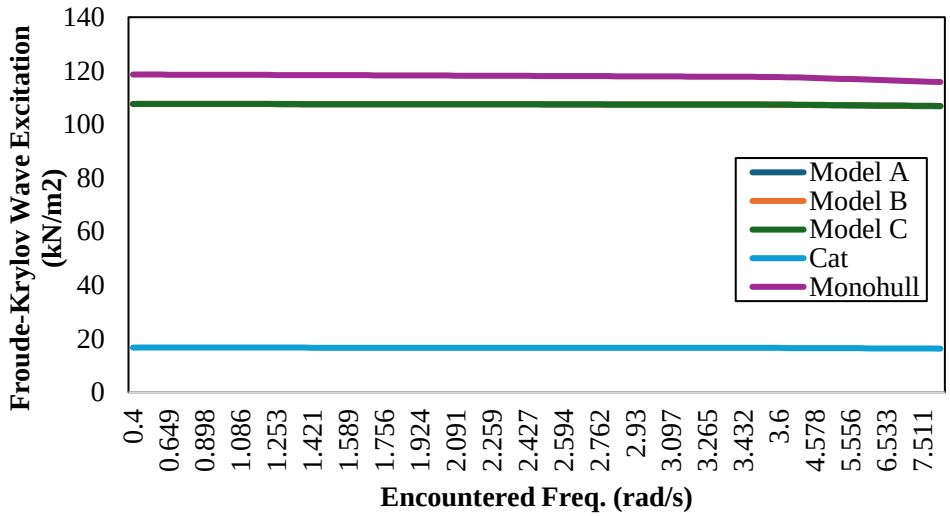

Figure 25. Froude-Krylov wave excitation (head sea) model a, b, c, catamaran, monohull in 5 knots

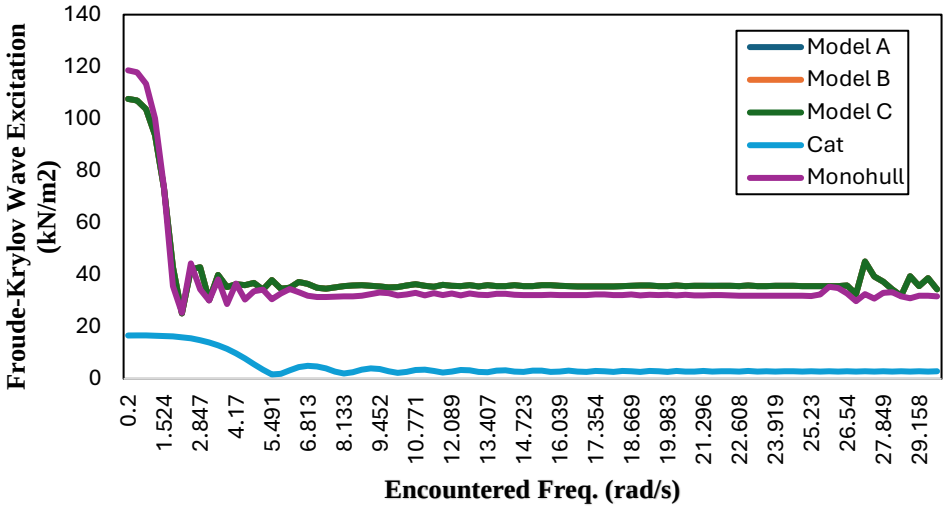

Figure 26. Froude-Krylov wave excitation (beam sea) model a, b, c, catamaran, monohull in 5 knots.

The graphs presented illustrate the dynamic responses of various ship models under the influence of encountered wave frequencies, with a particular focus on Froude-Krylov wave excitation forces in beam sea conditions. The Froude-Krylov force is a critical aspect of naval architecture, as it pertains to the direct pressure exerted by undisturbed incident waves on the hull of a vessel. This force is especially significant in beam sea conditions, where waves impact the side of the vessel, leading to potential rolling motions and overall stability challenges. The graphs reflect how different hull designs respond to these forces, providing insight into their performance in real-world sea conditions. Model A shows a pronounced response to lower wave frequencies, characterized by a high amplitude that gradually diminishes as the frequency increases. This indicates that Model A is particularly sensitive to longer, lower-frequency waves, which are common in many oceanic environments. Such sensitivity can lead to increased rolling motions and instability, especially in beam seas. In contrast, Models B and C, although they follow a similar response pattern to Model A, stabilize at a lower amplitude, suggesting that these designs have features that better mitigate the impact of Froude-Krylov forces. This could be due to design optimizations that reduce the wave excitation forces or enhance the damping characteristics of the hull.

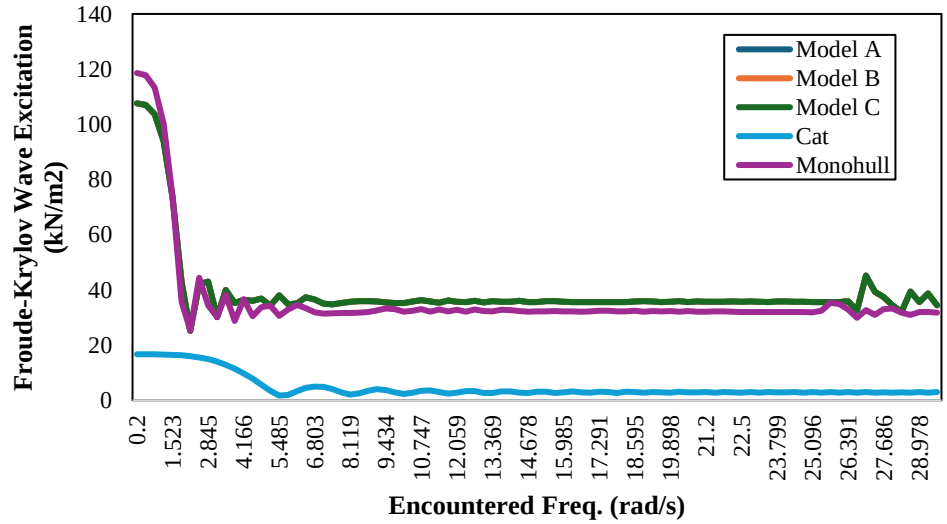

Figure 27. Froude-Krylov wave excitation (beam sea) model a, b, c, catamaran, monohull in 10 knots.

The catamaran model (Cat) demonstrates the lowest response across all encountered frequencies, highlighting the inherent stability advantages of multi-hull configurations in beam sea conditions. The twin-hull design likely disperses the wave forces more effectively, reducing the overall excitation and minimizing the vessel's rolling motion. On the other hand, the monohull design shows a high initial response, like Model A, but it stabilizes more quickly as the frequency increases. This suggests that while monohulls are vulnerable to low-frequency waves, they may perform better at higher frequencies, though not as effectively as the catamaran. The comparative analysis of these models underscores the importance of hull design in mitigating Froude-Krylov forces and ensuring vessel stability, particularly for ships operating in challenging sea conditions.

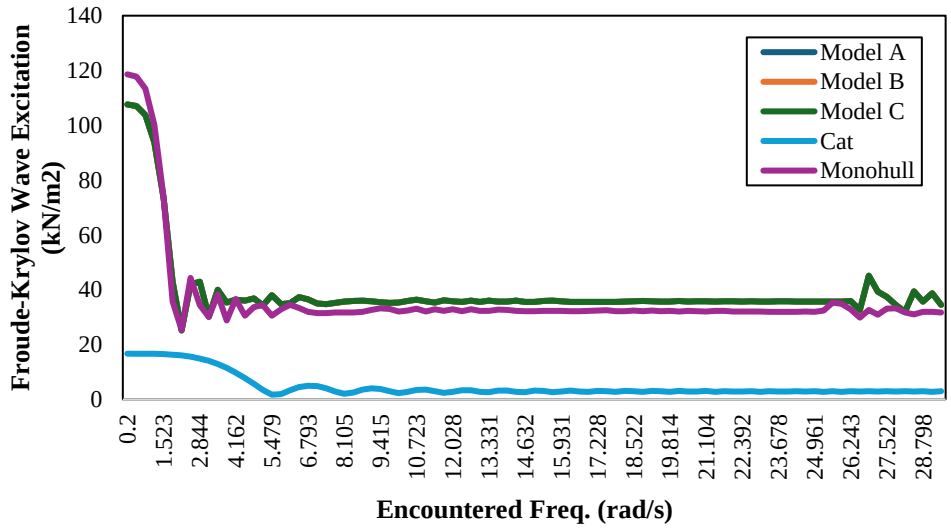

Figure 28. Froude-Krylov wave excitation (beam sea) model a, b, c, catamaran, monohull in 15 knots.

In summary, these graphs offer valuable insights into the dynamic behavior of different ship designs when subjected to beam sea conditions. The significant variation in responses among the models emphasizes the need for careful consideration of Froude-Krylov excitation forces in the design process. The catamaran's superior performance in maintaining low response levels across all frequencies suggests that multi-hull designs may offer enhanced stability and safety compared to traditional monohull designs, especially in environments characterized by beam seas. Understanding these dynamics is crucial for naval architects to optimize ship designs for stability, comfort, and safety in diverse maritime conditions.

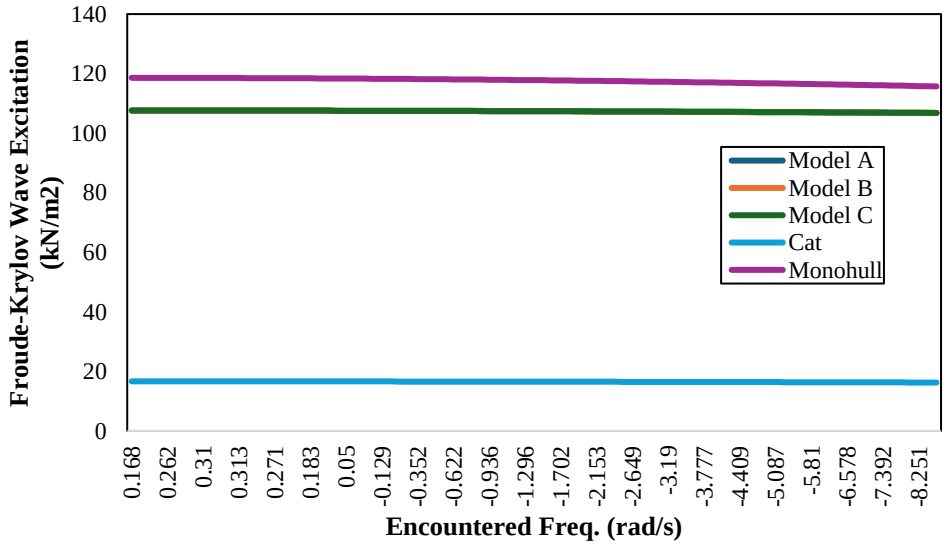

Figure 29. Froude-Krylov wave excitation (following sea) model a, b, c, catamaran, monohull in 15 knots.

The graphs illustrate the Froude-Krylov wave excitation in a following sea for different models: Model A, Model B, Model C, Cat, and Monohull. Across all graphs, Models A, B, and C consistently show the highest values, ranging from approximately 120 kN/m^2 to 140 kN/m^2, indicating a higher sensitivity to wave forces. These models maintain a flat line across the range of encountered frequencies, suggesting stable performance regardless of the frequency.

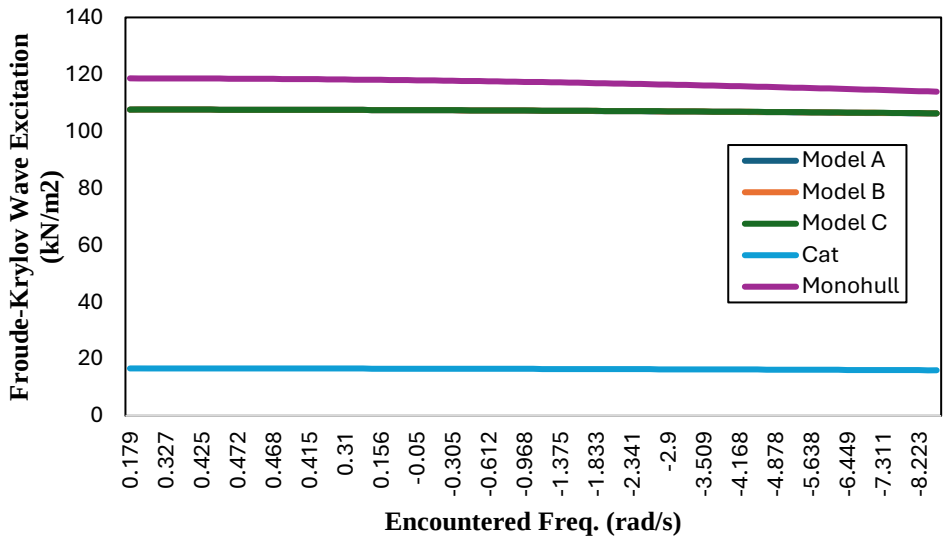

Figure 30. Froude-Krylov wave excitation phase (following sea) model a, b, c, catamaran, monohull in 10 knots.

The Cat model, with values around 100 kN/m^2, also demonstrates consistent performance across different frequencies. This model shows moderate wave excitation, positioning it between the higher sensitivity of Models A, B, and C, and the lower sensitivity of the Monohull model. The consistency in the Cat model's performance across the encountered frequencies indicates its reliability in a following sea.

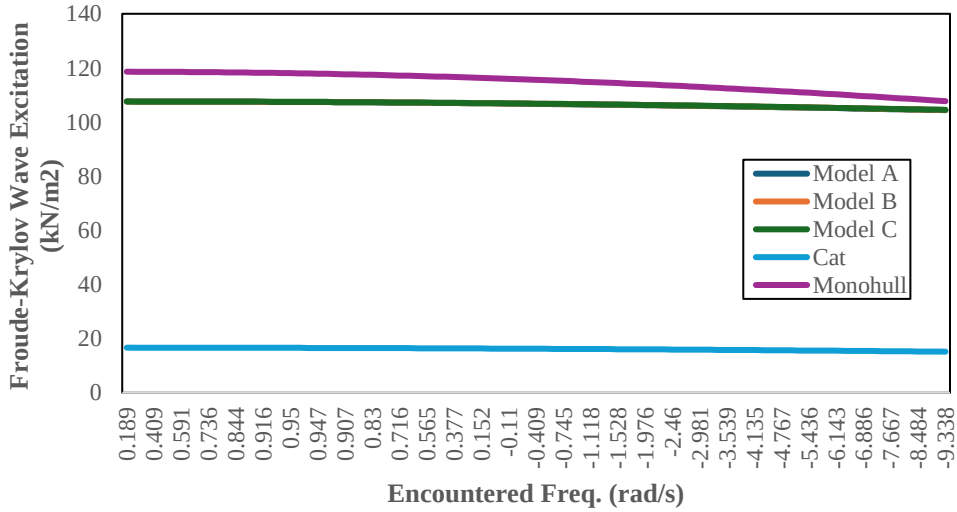

Figure 31. Froude-Krylov wave excitation (following sea) model a, b, c, catamaran, monohull in 5 knots.

The Monohull model stands out with the lowest values, close to 20 kN/m^2, indicating significantly lower wave excitation compared to the other models. Like the others, its performance remains consistent across the range of encountered frequencies. This suggests that the Monohull model might be less affected by wave forces in a following sea, making it potentially more stable in such conditions. Although STASH models tend to show lower wave excitation, the performance are still far from what have been expected by the absence of hull part in the middle (even not fully like catamaran). The performance of all STASH models more likely to be similar compared to monohull, even when the span was maximized like what it is in model A. Thus, a not significant change in performance (in the terms of

seakeeping and hydrodynamic force) is not truly functional and appealing for the naval architect to adopt a STASH hull design.

4. Conclusion

Based on the research findings, a variety of conclusions can be derived from the detailed analysis and comparative methods employed in simulating the hydrodynamic forces and seakeeping characteristics of single-to-twin after ship hulls (STASH). The study highlights that the factors influencing the performance, and the outcomes of the simulation can vary significantly. These factors include the specific design and motion features of each hull, the environmental conditions during the simulation, and the computational models used in the analysis. The research underscores the complexity and interdependence of these variables, suggesting that a comprehensive approach is necessary to accurately predict and enhance the performance of STASH configurations. The detailed conclusions drawn from the study are as follows. Compared to catamaran, STASH model seakeeping performance did not significantly perform better, while compared to monohull STASH only performed a bit better. In terms of seakeeping and hydrodynamic force, the modifications of STASH variants do not show any great change in performance. Thus, STASH cannot be recommended as a new better design or cluster.

References

[1] M. Sang Jin Kim, "The Inflluence Of Fluid Structure Interaction Modelling On The Dynamic Response Of Ship Subject To Collision And Grounding," *Marine Structures,* 2021.

[2] R. Bhattacharya, Dynamics Of Marine Vehicles, New York: A Wiley-Interscience Publication, 1978.

[3] Shahroz Khan, "Shiphullgan: A Generic Parametric Modeller For Ship Hull Design Using Deep Convolutional Generative Model," *Computer Methods In Applied Mechanics And Engineering,* 2023.

[4] Poundra, "Optimizing Trimaran Yacht Hull Configuration Based On Resistance And Seakeeping Criteria," In *Procedia Engineering*, 2017.

[5] C. Barrass, Ship Design And Performance For Masters And Mates, Burlington: Elsevier Science, 2004.

[6] Barrass, Ship Stability For Masters And Mates, Burlington: Elsevier Science, 2006.

[7] Amalia Ika Wulandari, "Numerical Analysis Of Ship Motion Of Crew Boat With Variations Of Wave Period On Ship Operational Speed," *CFD Letters,* Pp. 1-15, 2024.

[8] B. Systems, Maxsurf Motions Windows Version 20: User Manual, Bentley Systems, 2013.

[9] S. Lee, "Hydrodynamic Interaction Forces On Different Ship Types Under Various Operating Conditions In Restricted Waters," *Ocean Engineering,* 2023.

[10] M. K. Hakung Jang, "Effects Of Nonlinear FK (Froude - Krylov) And Hydrostatic Restoring Forces On Arctic-Spar Motions In Waves," *International Journal Of Naval Architecture And Ocean Engineering,* Vol. 12, Pp. 297 - 313, 2020.

[11] BMKG, "Pusat Meteorologi Maritim," Badan Meteorologi, Klimatologi Dan Geofisika, 10 06 2024. [Online]. Available: Https://Maritim.Bmkg.Go.Id/Prakiraan/Satu_Minggu_Kedepan. [Accessed 10 06 2024].

[12] R. H. Stewart, Introduction To Physical Oceanography, Texas: Texas A&M University, 2008.

[13] Sung-Jae Kim, "The Effects Of Geometrical Buoy Shape With Nonlinear Froude-Krylov Force On A Heaving Buoy Point Absorber," *International Journal Of Naval Architecture And Ocean Engineering,* Vol. 13, Pp. 86-101, 2021.

[14] Kenneth Weems, "Reduced-Order Model For Ship Motions Incorporating A Volume-Based Calculation Of Body-Non Linear Hydrostatic And Froude-Krylov Forces," *Ocean Engineering,* Vol. 289, No. 116214, 2023.

[15] A. Williams, "Froude-Krylov Force Coefficients For Bodies Of Rectangular Section In The Vicinity Of Free-Surface And Sea-Bed," *Ocean Engineering,* Vol. 21, No. 7, Pp. 663-682, 1994.

[16] Maxsurf, "Motions Seakeeping Performance Prediction," Bentley Engineering, 2024. [Online]. Available: Https://Maxsurf.Net/Motions-Seakeeping-Performance-Prediction. [Accessed 12 06 2024].

[17] J. Halkyard, Handbook Of Offshore Engineering, Illinois, USA: Elsevier Science, 2005.

[18] Tupper, Introduction To Naval Architecture (Fifth Edition), Butterworth-Heinemann, 2013.

[19] B. Systems, Maxsurf Motions: Windows Version 20 User Manual, Bentley Systems, Incorporated, 2013.

[20] Lars Larsson, Principles Of Yacht Design (Fifth Edition), Adlard Coles, 2022.

[21] Z. Junlei Cai, "Experimental And Numerical Study Of The Added Resistance And Seakeeping Performance Of A New Unmanned Survey Catamaran," *Ocean Engineering,* Vol. 308, No. 118255, 2024.

[22] Y. Thi Loan Mai, "Experimental Investigation On Wave Characteristics Due To Interference Of Catamaran Demi-Hulls In Waves," *International Journal Of Naval Architecture And Ocean Engineering,* Vol. 16, No. 100594, 2024.

[23] B. Kenneth Weems, "Reduced-Order Model For Ship Motions Incorporating A Volume-Based Calculation Of Body-Nonlinear Hydrostatic And Froude-Krylov Forces," *Ocean Engineering,* Vol. 289, No. 116214, 2023.

[24] Zhengyu Shi, "Multi-Degree-Of-Freedom Motions And Effect On Rolling Dynamics Of Damaged Ship In Oblique Waves," *Ocean Engineering,* Vol. 313, No. 119518, 2024.

[25] Xiao Zhou, "Real-Time Prediction Of Full-Scale Ship Maneuvering Motions At Sea Under Random Rudder Actions Based On Bilstm-SAT Hybrid Method," *Ocean Engineering,* Vol. 314, No. 119664, 2024.